

# Selective Dispersion of Large-Diameter Semiconducting Single-Walled Carbon Nanotubes with Pyridine-Containing Copolymers

Nicolas Berton, Fabien Lemasson, Angela Poschlad, Velimir Meded, Frank Tristram, Wolfgang Wenzel,\* Frank Hennrich, Manfred M. Kappes,\* and Marcel Mayor\*

*The purity of single-walled carbon nanotubes (SWNTs) is a key parameter for their integration in electronic, optoelectronic and photonic devices. Samples of pristine SWNTs are inhomogeneous in terms of electric behavior and diameter and contain a variety of amorphous carbon and catalyst residues. To obtain high performance devices, purification of SWNTs is required. Conjugated polymers have emerged as efficient solubilizing and sorting agents for small diameter SWNTs (HiPco tubes,  $0.7\text{ nm} < \text{Ø} < 1.1\text{ nm}$ ). Nevertheless, reports on polymers able to efficiently sort large diameter SWNTs with  $\text{Ø} > 1.1\text{ nm}$  are lacking. Several pyridine-containing copolymers were synthesized for this purpose and showed efficient and selective extraction of semiconducting large diameter SWNTs (PLV tubes,  $\text{Ø} > 1.1\text{ nm}$ ). High concentration and high purity suspensions are obtained without the use of ultracentrifugation, which gives an up-scaling potential of the method. The emission wavelength is in near infrared region around  $1550\text{ nm}$  and fits with broadly used telecommunication wavelength window. The processes taking place at the interface were simulated by a newly designed hybrid coarse-grain model combining density functional theory and geometrical calculation to yield insights into the wrapping processes with an unprecedented level of details for such large diameter SWNTs.*

---

Dr. N. Berton, Dr. F. Lemasson, Dr. V. Meded,  
F. Tristram, Prof. W. Wenzel, Dr. F. Hennrich,  
Prof. M. M. Kappes, Prof. M. Mayor  
Institute of Nanotechnology  
Karlsruhe Institute of Technology  
D-76021, Karlsruhe, Germany  
E-mail: wolfgang.wenzel@kit.edu; manfred.kappes@kit.edu;  
marcel.mayor@unibas.ch

Dr. N. Berton  
Present address: SPram/UMR 5819 (CEA, CNRS, UJF),  
CEA/INAC 17 rue des Martyrs, 38054, Grenoble, France

A. Poschlad, Dr. V. Meded  
Steinbuch Centre for Computing  
Karlsruhe Institute of Technology  
D-76128, Karlsruhe, Germany  
Prof. M. M. Kappes  
Institute of Physical Chemistry  
Karlsruhe Institute of Technology  
D-76128, Karlsruhe, Germany  
Prof. M. M. Kappes, Prof. Dr. M. Mayor  
DFG Center for Functional Nanostructures  
D-76028, Karlsruhe, Germany  
Prof. M. Mayor  
University of Basel  
Department of Chemistry  
CH-4056, Basel, Switzerland

## 1. Introduction

Single-walled carbon nanotubes (SWNTs) have attracted much attention due to their unique mechanical, thermal, electrical and optical properties.<sup>[1,2]</sup> As selective synthetic methods are lacking, as-produced SWNTs are currently available as a mixture in terms of their  $(n,m)$  chiral indices, specific diameters  $\varnothing$ , chiral angles  $\theta$  and corresponding fundamental properties including their metallic or semiconducting behavior. However, most applications require high purity samples with well-defined properties especially in electronics, optoelectronics and photonics.<sup>[3-7]</sup> Thus, finding efficient methods for selective sorting of SWNTs remains a major challenge.<sup>[8]</sup> Several separation techniques have been developed for this purpose, including dielectrophoresis,<sup>[9]</sup> density gradient centrifugation<sup>[10]</sup> or DNA-wrapping followed by ion-exchange chromatography.<sup>[11,12]</sup> One-pot extraction by selective dispersion using non-covalent functionalization is of particular interest due to the preservation of the physical properties of the tubes and the up-scaling potential of the method.

In particular, conjugated polymers have raised great interest for sorting of semiconducting nanotubes since they enable high concentrations of debundled SWNTs, fine-tuning of the dispersing properties through polymer design as well as easy processing of promising polymer/SWNTs hybrid materials.<sup>[13-18]</sup> A wide library of polythiophene, polyfluorene, polycarbazole and copolymers thereof has been investigated over the past few years and near-monochiral suspensions have been achieved in some cases in organic media.<sup>[13-16,19-24]</sup> Moreover, recent results demonstrated that this technique allows discrimination between right- and left-handed SWNTs.<sup>[25]</sup>

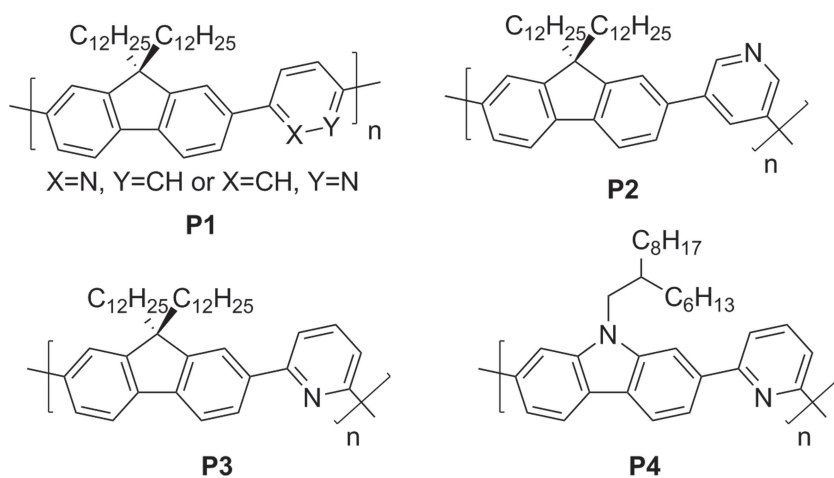
Despite these achievements, examples of single species extraction and more generally diameter-selectivity remain scarce. In particular there is still a lack of efficient polymers for dispersion of large-diameter SWNTs as research efforts have so far been mainly focused on the dispersion of SWNTs with relatively small diameter, i.e.,  $\varnothing < 1.2$  nm, from HiPco and CoMoCat materials. Pang et al. have shown that a poly(phenyleneethynylene-*co*-phenylenevinylene) polymer can disperse SWNTs with diameters up to 1.25 nm.<sup>[26]</sup> Our group recently reported the selective dispersion of large-diameter SWNTs, i.e., ca.  $\varnothing \approx 1.3$  nm using poly(9,9-didodecylfluorene-2,7-diyl-*alt*-anthracene-1,5-diyl),<sup>[27]</sup> thus reaching the diameter range that is highly desirable for near-infrared (near-IR) photonic applications, and in particular for optical communications.<sup>[28]</sup> Unfortunately, density gradient ultracentrifugation was necessary to efficiently remove the metallic species. At the same time, Tange et al. demonstrated that poly(9,9-dioctylfluorene-*alt*-benzothiadiazole) (F8BT) can extract SWNTs in the 1.3 to 1.4 nm diameter range, though at obviously low concentration.<sup>[29]</sup> Other recent studies also report polymer-assisted

dispersion of large-diameter SWNTs though the composition of the dispersion was unfortunately not studied in details.<sup>[30,31]</sup> These early results clearly point towards the need for further improvements of the extraction yield and selectivity for the development of practical applications in this diameter range.<sup>[32]</sup> The electron-rich pyridine group is able to form halogen and hydrogen-bonds and is widely used in supramolecular chemistry as ligand or as molecular clip in combination with metal complexes.<sup>[33-35]</sup> Incorporating pyridine groups in rod-coil block copolymers has also emerged as a promising way of controlling the nanostructure of organic solar cell thin films through charge-transfer complexation with electron-accepting fullerenes.<sup>[36-38]</sup> Surprisingly, pyridine has hardly been investigated in the context of SWNTs sorting, and so far only with small-diameter CoMoCat SWNTs.<sup>[39]</sup>

Here, we report on the dispersing properties of a family of pyridine-containing copolymers which were synthesized for this purpose. Efficient and selective one-pot extraction of large-diameter semiconducting SWNTs in toluene is obtained, with a diameter of  $\approx 1.25$  nm. These exhibit an emission wavelength centered at 1550 nm, which perfectly fits the range of the broadly used telecommunication C-band wavelength thus allowing direct application in photonics. Moreover, the selection process has been investigated using a newly developed hybrid coarse-grained model combining DFT and geometry-based calculations to model the wrapping mechanism taking place at large diameter SWNT/polymer interface at an unprecedented level of detail.

## 2. Results and Discussion

The investigated polymers constitute a family of four strictly alternating pyridine-containing copolymers and were synthesized using Suzuki cross-coupling polycondensation (see Scheme S1 in the Supporting Information). As depicted in **Scheme 1**, polymers **P1-P3** are three poly(fluorene-*alt*-pyridine) copolymers each with 2,7-linked fluorene units but varying by the connectivity of the pyridyl group. Note that polymer **P1** comprises pyridine-2,5-diyl an asymmetric building block missing a mirror plane with respect to its



**Scheme 1.** Structure of copolymers **P1-P4**.

connectivity. The orientation of the pyridine-2,5-diyl subunit was not controlled and thus the resulting polymer **P1** can be described as regiorandom with respect to the orientation of the pyridine subunit. In contrast to that, polymers **P2** and **P3** are assembled from exclusively symmetric building blocks resulting in strictly regioregular copolymers. Polymer **P4** is the carbazole-analogue of the parent fluorene copolymer **P3**.

The dispersing properties of polymers **P1–P4** were first studied using small-diameter (0.75–1.3 nm) HiPco SWNTs. The dispersions were obtained by ultrasonication of 1 mg of pristine SWNTs and 50 mg of the desired polymer in 15 mL of toluene with a titanium sonotrode followed by centrifugation with a mild centripetal acceleration of 5000g for 10 min to remove large nanotube bundles and remaining catalyst particles according to an established procedure as described in the Supporting Information. The SWNTs dispersions were analyzed by absorption and photoluminescence-excitation (PLE) spectroscopy and corresponding PLE  $\theta/\emptyset$  maps were generated from the data sets to visualize the composition of the dispersed SWNTs in each suspension. The  $(n,m)$  distribution of SWNTs in HiPco raw material being non-uniform, relative PLE  $\theta/\emptyset$  maps are also presented in order to give a better estimate of the polymer extraction ability. Relative PLE  $\theta/\emptyset$  maps show the ratio between the PLE intensity of a  $(n,m)$  specie obtained using polymer extraction and the intensity obtained using the non selective dispersant sodium cholate in  $D_2O$ . We note that the accuracy of such relative intensity maps is likely to be lower in regions of higher diameters due to the correspondingly low amount of SWNTs present.<sup>[40]</sup> Finally, note that PLE spectroscopy exclusively detects semiconducting SWNTs, whereas both metallic and semiconducting tubes are observed by absorption spectroscopy. Thus the displayed PLE  $\theta/\emptyset$  maps only represent the relative fractions of semiconducting tubes for samples in which metallic tubes can also be present.

**Figure 1** displays the PLE  $\theta/\emptyset$  maps obtained with the pyridine based copolymers **P1–P4** as well as the corresponding  $\theta/\emptyset$  maps and relative  $\theta/\emptyset$  maps. As evidenced by these latter maps, polymers **P1–P4** display tunable diameter-selective features depending upon the connectivity of the pyridine unit. A comparison between suspension **P1**/SWNTs in figure 2g and the pristine HiPco SWNTs composition displayed in figure 2f<sup>[27]</sup> shows that polymer **P1** is able to disperse all semiconducting SWNTs species present in the HiPco materials. Both high PLE intensities (Figure 1b) and high absorbance values (**Figure 2**) measured for the **P1**/SWNTs dispersion are indicative of a relatively high concentration of SWNTs compared to the SWNT suspensions prepared from **P2–P4**. The strong absorption background and the presence of signals in the  $M_{11}$  absorption band (400–600 nm) indicate the presence of metallic species. Thus, polymer **P1** is a very efficient but non-selective dispersing agent for HiPco SWNTs in toluene. Polymer **P2** partially discriminates against low-diameter species with  $\emptyset < 0.9$  nm, in particular the (6,5), (7,5) and (8,3) species (Figure 1c,h,m). However most species remain detectable in the dispersion to some degree, and therefore the low absorbance (Figure 2) and very low PLE peak intensities recorded point more towards poor dispersing properties of the polymer in general than to its high selectivity. Interestingly a pronounced selectivity for

large-diameter SWNTs having  $\emptyset > 1.0$  nm was observed for polymer **P3**. In this case the low PLE (Figure 1d) and absorbance intensities (Figure 2) arise from the fact that the dispersed species constitute only a very minor part of the parent HiPco SWNT mixture folded with the strong selectivity of **P3** as shown by its relative  $\theta/\emptyset$  map in figure 1n. Furthermore, the low background and the absence of characteristic signals within the detection threshold of metallic tubes in the  $M_{11}$  absorption band of the absorption spectrum of the **P3**/HiPco SWNTs dispersion indicate an exclusive extraction of semiconducting species. As a first working hypothesis these promising selection features of the copolymer **P3** were attributed to its 2,6-connected pyridine subunit. Unfortunately this first design hypothesis turns out to be much too simple as the carbazole-containing homologue **P4** does not exhibit similar dispersion properties and only a minor tendency to discriminate small SWNTs with  $\emptyset < 0.9$  nm was observed (Figure 1e,j,o). According to our current working hypothesis, this overall behavior can be attributed to subtle structural changes induced by the  $sp^2$  hybridization of the N-bridging atom of the carbazole unit which induce a variation in the angle formed by the two bonds in para-position.<sup>[19,23]</sup>

The ability of these polymers to disperse large-diameter SWNTs was then studied using SWNTs synthesized by PLV, which are known to have a mean diameter of  $\approx 1.3$  nm.<sup>[41,42]</sup> PLE spectroscopy measurements for **P3**/PLV SWNTs dispersed in toluene reveal that polymer **P3** extracts SWNTs having a diameter up to 1.3 nm, with the (10,9), (10,8), (11,7) and (13,5) SWNTs as the main species (**Figure 3**). No  $\theta$ -selectivity is observed as low-chiral angle  $\theta$  species (15,1) and (14,3) are also extracted. The emission wavelengths of these SWNTs are distributed within  $1450 < \lambda < 1600$  nm (Figure 3). Relatively similar distributions were observed with polymers **P1**, **P2** and **P4** (Figure S2), although the carbazole-containing polymer **P4** seems slightly more selective toward high- $\theta$  SWNTs (Figure S2). The largest SWNT identified, i.e., the (13,6) species, has a diameter of 1.32 nm. Most likely, even larger-diameter species were dispersed in these samples but could not be detected by PLE spectroscopy due to the recording window of our PL spectrometer as well as due to the solvent absorption. Most importantly, the low background and the absence of any signal in the  $M_{11}$  absorption band (600–700 nm) of the absorption spectra of dispersions obtained using polymers **P3** and **P4** clearly documents the selective extraction of semiconducting SWNT species (**Figure 4**),<sup>[12]</sup> while metallic nanotubes are still present in the **P1**/PLV SWNTs and **P2**/PLV SWNTs dispersions, as was already observed with HiPco SWNTs (vide supra). The characteristic signals of semiconducting SWNTs can be well identified in the  $S_{33}$ ,  $S_{22}$ , and  $S_{11}$  absorption bands at 500–600 nm, 800–1200 nm, and 1500–1900 nm, respectively. This result represents a significant improvement over our previously reported fluorene-*alt*-anthracene copolymer that required a subsequent density gradient centrifugation (DGC) step to remove metallic traces.<sup>[27]</sup> According to absorbance intensities, the highest concentration of pure large-diameter semiconducting SWNTs was obtained with polymer **P3**. It was also verified that the concentration of large-diameter semiconducting SWNTs in the **P3**/PLV SWNTs dispersion is

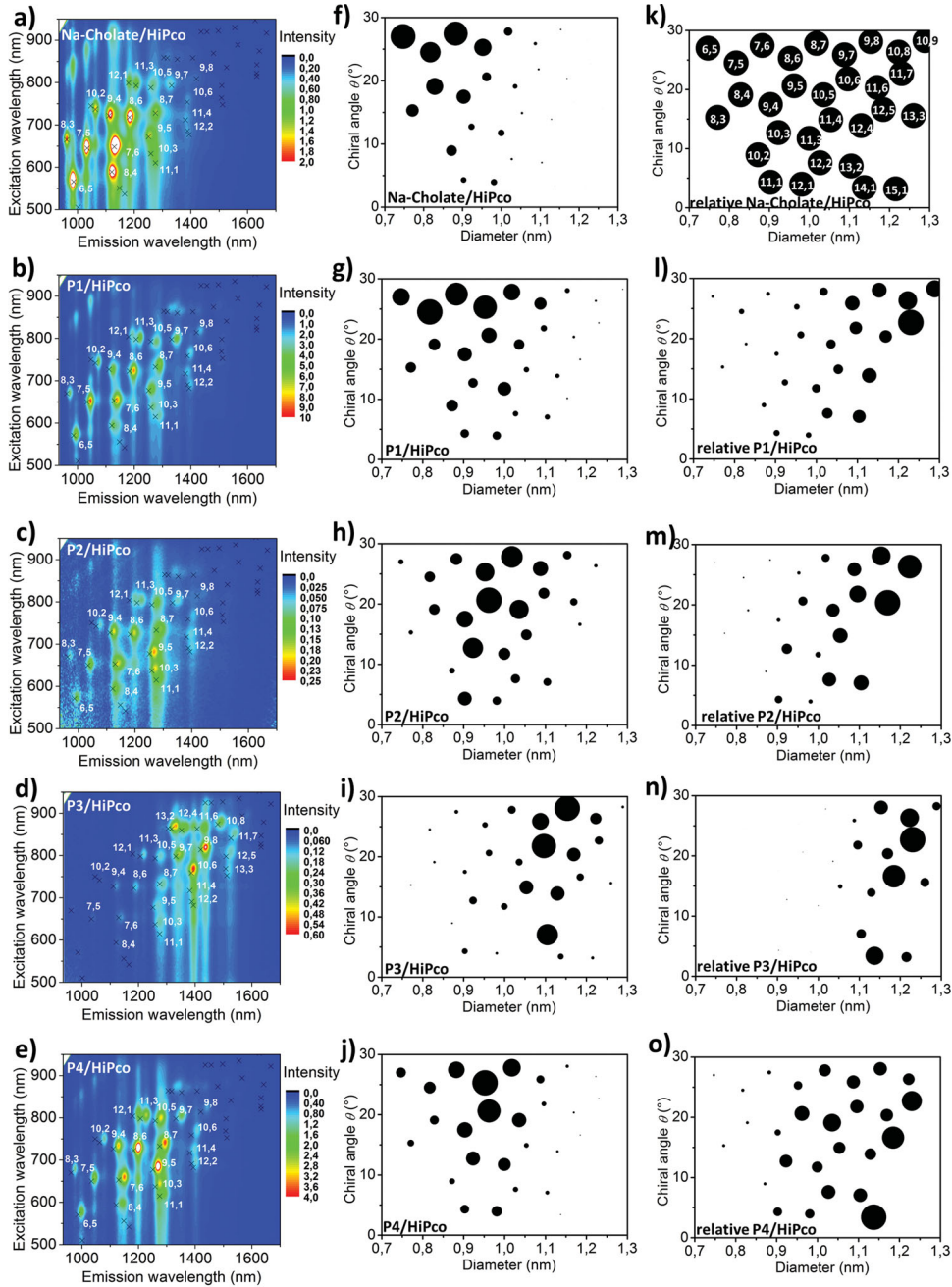


**Figure 1.** a) PLE map of HiPco SWNTs dispersed using sodium cholate in  $D_2O$ . b-e) PLE maps of HiPco SWNTs dispersed using polymers **P1–P4** in toluene, respectively. f-j) Corresponding  $\theta/\phi$  maps derived from the PLE maps presented in a-e, respectively. Within an individual  $\theta/\phi$  map the area of each circle is proportional to the PL intensity of the single  $(n,m)$ -SWNT specie. k-o) Relative  $\theta/\phi$  maps representing the ratio between the PL intensity of a single polymer wrapped  $(n,m)$ -SWNT specie and its reference PL intensity in aqueous sodium cholate suspension.

much higher than the concentration obtained under similar conditions using polymer PDDF-BT (Figure S3), a parent of polymer F8BT previously reported by Tange et al.<sup>[29]</sup> The overall extraction yield of semiconducting SWNTs can be estimated to be as high as 70% (see Table S1). These properties further increase the interest in these new pyridine-containing polymers for selective and efficient extraction of large-diameter SWNTs, especially in view of photonic applications.<sup>[28]</sup> Thus, copolymer **P3**, with its 2,6-connected pyridine unit, appears to be a promising candidate for diameter-selective extraction.

### 3. Theoretical Investigations

Previously, an opposite trend was reported for poly(flourenalt-bipyridine) which contains a 2,6-linked bipyridine group instead of a pyridine group. This was found to extract only very small-diameter SWNTs. The accompanying molecular dynamics (MD) simulations mostly failed to explain the phenomenon.<sup>[39]</sup> Also several other approaches to model polymer/SWNTs structures have been inconclusive in their description of the complex systems at hand.<sup>[20]</sup> As observed in our previous work on SWNT/polymer structures<sup>[19]</sup> as

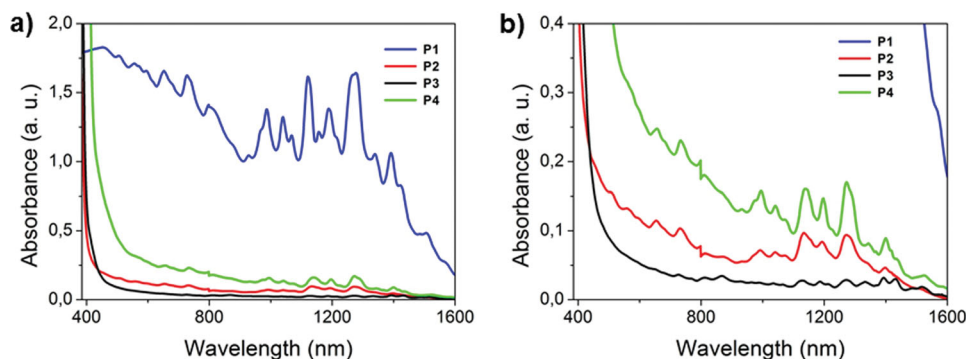


**Figure 2.** a) Absorbance spectra of HiPco SWNTs dispersions in toluene prepared using polymers **P1–P4**. b) Five fold enhancement of the absorbance spectra (a).

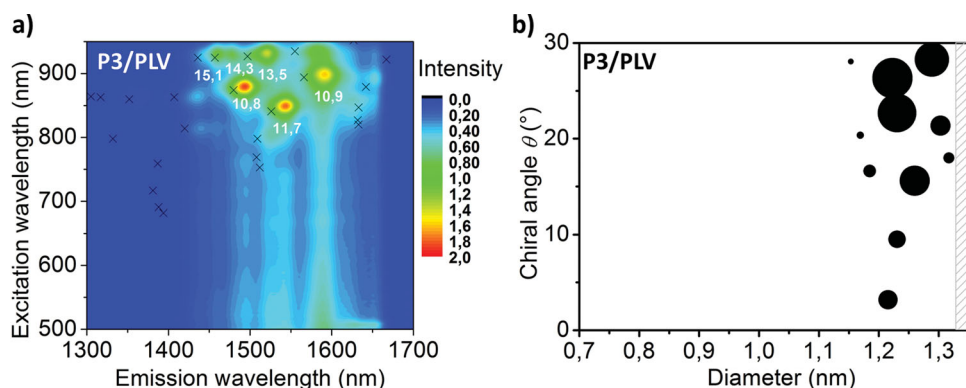


**Figure 3.** a) PLE map and b) corresponding  $\theta/\varnothing$  maps of polymer **P3**/PLV SWNTs dispersed in toluene. Potentially dispersed semiconducting SWNTs with even larger diameters (dashed grey area) are hidden by the solvents optical properties.

well as by other groups,<sup>[43,44]</sup> MD simulations converge very slowly and often fail to fully wrap the SWNT. To circumvent these convergence problems we have developed a coarse-grained model which abstracts from the chemical details and treats both tube and polymer units as geometrical objects.

The approach, assumes that maximal (attractive)  $\pi$ - $\pi$  interactions can be reached by maximizing the contact area between SWNT and the wrapping polymer, i.e., it constructs

a set of solutions for which the polymer lies flat on the tube (for details see the Supporting Information) according to Equation (1):

$$E_{tot} = E_{pd} + E_{pr} + E_{pNT} + E_{NT} \approx E_{pd} + const. \quad (1)$$

where  $E_{tot}$  is the total energy,  $E_{pd}$  is the polymer dihedral angle energy contribution,  $E_{pr}$  is the rest of the polymer total energy,  $E_{pNT}$  represents the polymer–nanotube interaction energy and  $E_{NT}$  is the nanotube total energy.

In order to construct these sets of mathematically possible wrapping solutions, the energy of a dimer was first calculated using ab initio methods<sup>[45]</sup> according to the two dihedral angles alpha and beta formed by the fluorene (or carbazole) and the pyridine plans (**Figure 5a**). These angles are the two main degrees of conformational freedom in the polymer backbone. Note that the alkyl chains are not considered in the calculations and were translated into methyl groups. The calculations were performed for a polymer length of 12 repeating units for polymers **P2–P4**, and only 9 repeating units for polymer **P1** in order to fit with its experimental length. The solutions are scored according to the dihedral potential energy of the polymer (Figure S6) as calculated with ab-initio DFT methods using the B3-LYP exchange correlation functional (Figure 5b).<sup>[46]</sup> The dihedral potential energy of polymers **P1–P4** was calculated for 7 different tube diameters, specifically 0.72, 0.8, 0.9, 1.0, 1.1, 1.2, and 1.25 nm. Solutions having lower dihedral potential energy are assumed to be more likely

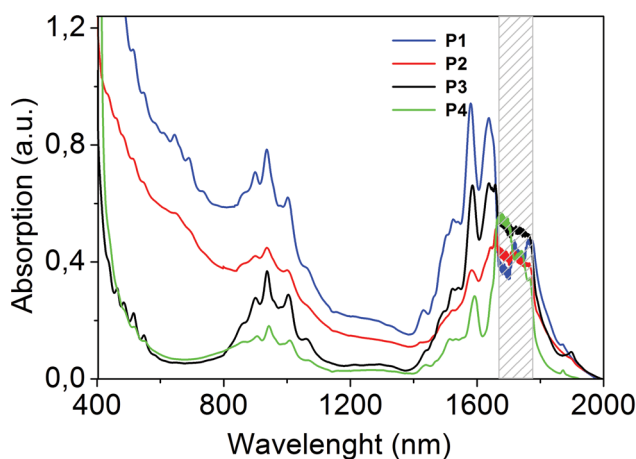


**Figure 4.** Absorbance spectra of PLV SWNTs dispersions prepared using polymers **P1–P4** in toluene. The dashed grey zone indicates the absorption of the solvent (toluene), which precludes any inferences concerning SWNTs in this wavelength window (1670–1770 nm).

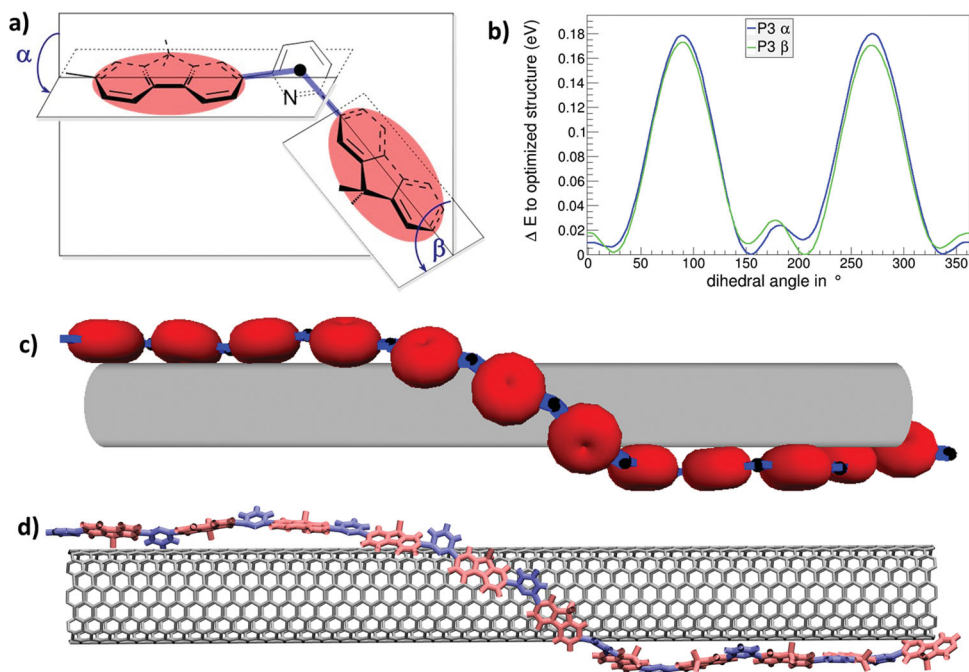


**Figure 5.** a) Geometrical representation of polymer **P3**. The fluorene or carbazole moieties in polymers **P1–P4** are represented by red discs which are centered at the intersection of the outgoing bonds. The pyridine moieties are indicated by black dots. These two types of objects are connected by sticks whose lengths reflect the bonds between the fluorene or carbazole moiety and the distance to the center of pyridine ring. b) Energy profile of the rotatable dihedral angles labeled as  $\alpha$  and  $\beta$  for **P3** as obtained by (vacuum) DFT calculations. c) Example solution calculated for polymer **P3** containing 12 repeating units and wrapping a cylinder with a diameter of 1.2 nm. d) The solution represented in (c) is translated into a molecular model. The alkyl chains are simplified as methyl groups.

to form. Since the polymers act on different energy scales (see Figure S7) with vastly different numbers of solutions possible per polymer, an energy cut-off was chosen for each polymer separately. Thus, the number of solutions considered for

polymers **P1–P4** is 30, 40, 30 and 15 respectively. Figure 5c,d represent one of the solutions for polymer **P3** depicted as coarse-grained model around a cylinder of 1.2 nm diameter and translated as molecular model around a 1.2 nm SWNT, respectively. The number of solutions for polymer **P1–P4** were normalized and plotted in **Figure 6** together with the normalized relative intensity of SWNTs dispersed by **P1–P4** obtained experimentally and displayed in Figure 1i–o.

The conformations (and their relative energies) as obtained by our model generally capture the experimental data well. For polymer **P1**, Figure 6a shows the solutions distributed over the corresponding diameters. The number of favorable solutions increases together with increasing diameter to reach a maximum at a diameter of 1.2 nm. In case of polymer **P2**, a few low-energy solutions were found at small diameter SWNTs thus overestimating the experimental findings (Figure 6b). For polymer **P3**, the highest relative abundance of low energy solutions is seen to range from 0.9 to 1.3 nm diameter with a maximum at 1.2 nm (Figure 6c). Favorable solutions for polymer **P3** are clearly most commonly found for large diameter tubes, which is in good agreement with the experimental data. Finally, according to our simulations, polymer **P4**

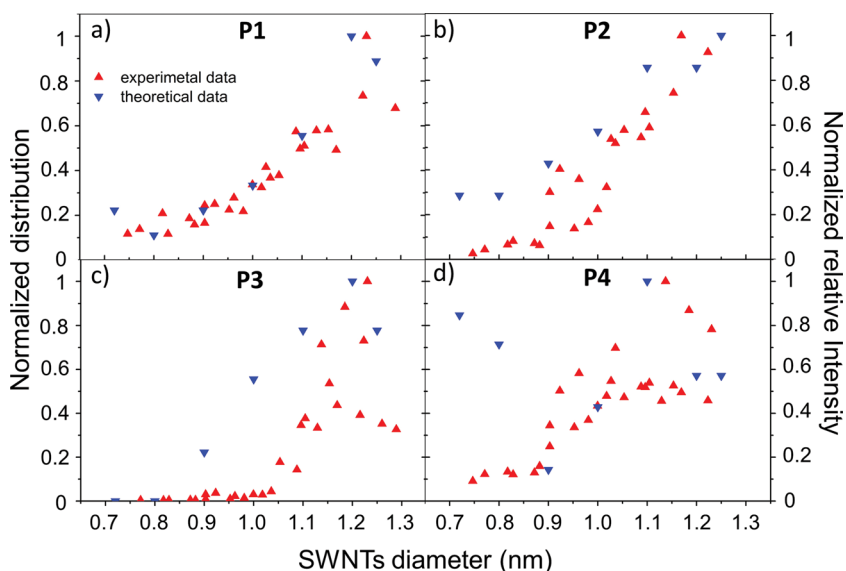


**Figure 6.** a-d) Comparison of experimental results and theoretical calculations for extracted SWNTs using polymers **P1–P4**, respectively, according to the diameter. Normalized relative intensities of SWNTs dispersed by **P1–P4** are extracted from figure 1 and are represented by red triangles. The fraction of “lowest energy” constructed solutions for **P1–P4** is normalized and represented with upside down blue triangles (see the Supporting Information for more details).

prefers SWNTs with 1.0 nm diameter and above as well as SWNTs with diameters smaller than 0.8 nm, thus forming a gap between 0.8 and 1.0 nm. The experiment, on the other hand, displays only a drop below 1.0 nm (Figure 6d).

The solution abundance distributions predicted by our model agree well with the experimental relative PL intensities displayed by polymers **P1–P4**. Thus the parameters of our simple model (variable dihedral profiles and fixed bond angles) are apparently able to rationalize the different selectivity observed. The connectivity of the pyridine unit for polymers **P1–P3** appears decisive. The pyridine ring is connected in 1,4-, 2,4- and 1,5- positions which gives rise to bond angles of 177.6°, 121.8°, and 115°, respectively.<sup>[20]</sup> The smallest angle leads to maximum exclusion of small diameter tubes. The angle difference between polymers **P3** and **P4** stems from the intrinsic difference between fluorene (polymer **P3**, angle 160.6°) and carbazole (**P4**, angle 156.2°) groups. Minimizing this angle seems to allow wrappings of smaller diameter SWNTs, thus degrading the polymer selectivity toward large diameter tube.

The coarse grained model appears to be a suitable alternative to construct possible solutions for polymer wrapping of SWNTs up to  $\varnothing \leq 1.3$  nm. Interestingly, although this model exclusively considers the arrangement of the polymer on the tube and ignores the precise position of tube atoms with respect to the coating polymer, it provides an impressive match with the found diameter selectivity. While this is encouraging on the one hand, the approach inherently excludes the description of structurally more detailed selection according to particular (*n,m*) indices or chiralities. Refinements in MD simulations will be performed in order to address such challenges in future.

## 4. Conclusion

In summary, a new family of fluorene and carbazole-based copolymers containing pyridine groups was synthesized and successfully used for selective dispersion of large-diameter SWNTs. In particular, poly(9,9-didodecylfluorene-2,7-diyl-*alt*-pyridine-2,6-diyl) **P3** exhibits diameter-selectivity toward semiconducting SWNTs with diameter >1 nm. Large-diameter semiconducting SWNTs with diameter up to ~1.3 nm were isolated in unprecedentedly high concentrations and semiconducting tube purities by one-pot extraction in toluene without need for further ultracentrifugation. Their emission properties correspond to the highly used optical fiber telecommunication wavelength at around 1550 nm. Thus, we provide a convenient and potentially up-scalable way to access these highly desired SWNTs. Furthermore, a novel coarse-grained model based on differences in energetic contributions of rotations of the corresponding dihedral angles was presented for the first time. It displays results which are in good qualitative agreement with the experimental findings and appears applicable for SWNT diameter of at least 1.3 nm. The reported findings may pave the way toward efficient low-cost extraction of large-diameter semiconducting SWNTs specifically targeted for new applications such as optical communications and photonics.

## Supporting Information

Supporting Information is available from the Wiley Online Library or from the author.

## Acknowledgements

We acknowledge ongoing generous support by the DFG Center for Functional Nanostructures (CFN), by the Helmholtz Programm POF NanoMikro, by the Karlsruhe Institute of Technology (KIT), the University of Basel, the bwGRiD project (the computing grid of the Baden Württemberg state) and the FP7 EU project MMM@HPC.

- [1] P. Avouris, M. Freitag, V. Perebeinos, *Nat. Photonics* **2008**, *2*, 341.
- [2] Q. Cao, J. A. Rogers, *Adv. Mater.* **2009**, *21*, 29.
- [3] S. Berger, C. Voisin, G. Cassabois, C. Delalande, P. Roussignol, *Nano Lett.* **2007**, *7*, 398.
- [4] N. IZARD, S. Kazaoui, K. Hata, T. Okazaki, T. Saito, S. Iijima, N. Minami, *Appl. Phys. Lett.* **2008**, *92*, 243112.
- [5] E. Gaufrès, N. IZARD, X. Le Roux, S. Kazaoui, D. Marris-Morini, E. Cassan, L. Vivien, *Opt. Express* **2010**, *18*, 5740.
- [6] S. Park, H. W. Lee, H. Wang, S. Selvarasah, M. R. Dokmeci, Y. J. Park, S. N. Cha, J. M. Kim, Z. Bao, *ACS Nano* **2012**, *6*, 2487.
- [7] Y. Asada, F. Nihey, S. Ohmori, H. Shinohara, T. Saito, *Adv. Mater.* **2011**, *23*, 4631.
- [8] M. C. Hersam, *Nat. Nanotechnol.* **2008**, *3*, 387.
- [9] R. Krupke, F. Hennrich, H. von Loehneysen, M. M. Kappes, *Science* **2003**, *301*, 344.
- [10] M. S. Arnold, A. A. Green, J. F. Hulvat, S. I. Stupp, M. C. Hersam, *Nat. Nanotechnol.* **2006**, *1*, 60.
- [11] M. Zheng, E. D. Semke, *J. Am. Chem. Soc.* **2007**, *129*, 6084.
- [12] X. Tu, S. Manohar, A. Jagota, M. Zheng, *Nature* **2009**, *460*, 250.
- [13] N. Stürzl, F. Hennrich, S. Lebedkin, M. M. Kappes, *J. Phys. Chem. C* **2009**, *113*, 14628.
- [14] J. Y. Hwang, A. Nish, J. Doig, S. Douven, C. W. Chen, L. C. Chen, R. J. Nicholas, *J. Am. Chem. Soc.* **2008**, *130*, 3543.
- [15] A. Nish, J. Y. Hwang, J. Doig, R. J. Nicholas, *Nat. Nanotechnol.* **2007**, *2*, 640.
- [16] F. Chen, B. Wang, Y. Chen, L. J. Li, *Nano Lett.* **2007**, *7*, 3013.
- [17] D. H. Kim, H. J. Shin, H. S. Lee, J. Lee, B. L. Lee, W. H. Lee, J. H. Lee, K. Cho, W. J. Kim, S. Y. Lee, J. Y. Choi, J. M. Kim, *ACS Nano* **2012**, *6*, 662.
- [18] H. W. Lee, Y. Yoon, S. Park, J. H. Oh, S. Hong, L. S. Liyanage, H. Wang, S. Morishita, N. Patil, Y. J. Park, J. J. Park, A. Spakowitz, G. Galli, F. Gygi, P. H. S. Wong, J. B. H. Tok, J. M. Kim, Z. Bao, *Nat. Commun.* **2011**, *2*, 541.
- [19] F. A. Lemasson, T. Strunk, P. Gerstel, F. Hennrich, S. Lebedkin, C. Barner-Kowollik, W. Wenzel, M. M. Kappes, M. Mayor, *J. Am. Chem. Soc.* **2011**, *133*, 652.
- [20] H. Ozawa, T. Fujigaya, Y. Niidome, N. Hotta, M. Fujiki, N. Nakashima, *J. Am. Chem. Soc.* **2011**, *133*, 2651.
- [21] H. Ozawa, T. Fujigaya, S. Song, H. Suh, N. Nakashima, *Chem. Lett.* **2011**, *40*, 470.
- [22] W. Z. Wang, W. F. Li, X. Y. Pan, C. M. Li, L.-J. Li, Y. G. Mu, J. A. Rogers, M. B. Chan-Park, *Adv. Funct. Mater.* **2011**, *21*, 1643–1651.
- [23] F. Lemasson, N. Berton, J. Tittmann, F. Hennrich, M. M. Kappes, M. Mayor, *Macromolecules* **2012**, *45*, 713.
- [24] P. Gerstel, S. Klumpp, F. Hennrich, O. Altintas, T. R. Eaton, M. Mayor, C. Barner-Kowollik, M. M. Kappes, *Polym. Chem.* **2012**, *3*, 1966.

- [25] K. Akazaki, F. Toshimitsu, H. Ozawa, T. Fujigaya, N. Nakashima, *J. Am. Chem. Soc.* **2012**, *134*, 12700.
- [26] Y. Chen, A. Malkovskiy, X. Q. Wang, M. Lebron-Colon, A. P. Sokolov, K. Perry, K. More, Y. Pang, *ACS Macro Lett.* **2012**, *1*, 246.
- [27] N. Berton, F. Lemasson, J. Tittmann, N. Stürzl, F. Hennrich, M. M. Kappes, M. Mayor, *Chem. Mater.* **2011**, *23*, 2237.
- [28] T. Hasan, Z. Sun, F. Wang, F. Bonaccorso, P. H. Tan, A. G. Rozhin, A. C. Ferrari, *Adv. Mater.* **2009**, *21*, 3874.
- [29] M. Tange, T. Okazaki, S. Iijima, *J. Am. Chem. Soc.* **2011**, *133*, 11908.
- [30] H. Wang, J. Mei, P. Liu, K. Schmidt, G. Jimenez-Oses, S. Osuna, L. Fang, C. J. Tassone, A. P. Zoombelt, A. N. Sokolov, K. N. Houk, M. F. Toney, Z. Bao, *ACS Nano* **2013**, *7*, 2659.
- [31] C. Wang, L. Qian, W. Xu, S. Nie, W. Gu, J. Zhang, J. Zhao, J. Lin, Z. Chen, Z. Cui, *Nanoscale* **2013**, *5*, 4156.
- [32] During the writing of our manuscript, a study comprising a fluorene-bipyridine copolymer described a one pot extraction yielding high concentrated suspension of semiconducting large diameter SWNTs without the need of DGC treatment. Nevertheless, no theoretical investigation was performed in this work: K. S. Mistry, B. A. Larsen, J. L. Blackburn, *ACS Nano* **2013**, *7*, 2231.
- [33] A. C. C. Carlsson, J. Grafenstein, A. Budnjo, J. L. Laurila, J. Bergquist, A. Karim, R. Kleinmaier, U. Brath, M. Erdelyi, *J. Am. Chem. Soc.* **2012**, *134*, 5706.
- [34] F. D'Souza, A. N. Amin, M. E. El-Khouly, N. K. Subbaiyan, M. E. Zandler, S. Fukuzumi, *J. Am. Chem. Soc.* **2012**, *134*, 654.
- [35] V. L. Gunderson, A. L. Smeigh, C. H. Kim, D. T. Co, M. R. Wasielewski, *J. Am. Chem. Soc.* **2012**, *134*, 4363.
- [36] A. Laiho, R. H. A. Ras, S. Valkama, J. Ruokolainen, R. Österbacka, O. Ikkala, *Macromolecules* **2006**, *39*, 7648.
- [37] N. Sary, F. Richard, C. Brochon, N. Leclerc, P. Lévêque, J. N. Audinot, S. Berson, T. Heiser, G. Hadziioannou, R. Mezzenga, *Adv. Mater.* **2010**, *22*, 763.
- [38] C. Renaud, S. J. Mougner, E. Pavlopoulou, C. Brochon, G. Fleury, G. Deribew, G. Portale, E. Cloutet, S. Chambon, L. Vignau, G. Hadziioannou, *Adv. Mater.* **2012**, *24*, 2196.
- [39] H. Ozawa, N. Ide, T. Fujigaya, Y. Niidome, N. Nakashima, *Chem. Lett.* **2011**, *40*, 239.
- [40] Indeed, the signal of few large diameter SWNTs in the PLE map measured from the sodium cholate/HiPco SWNTs suspension were below the detection threshold. For these SWNTs, we have attributed a value of 1% of the highest PLE signals.
- [41] S. Lebedkin, F. Hennrich, T. Skipa, M. M. Kappes, *J. Phys. Chem. B* **2003**, *107*, 1949.
- [42] J. P. Yang, M. M. Kappes, H. Hippler, A. N. Unterreiner, *Solid State Phenomena Vols* **2007**, *121–123*, 905.
- [43] J. Gao, M. A. Loi, E. J. Figueiredo de Carvalho, M. C. dos Santos, *ACS Nano* **2011**, *5*, 3993.
- [44] J. K. Sprafke, S. D. Stranks, J. H. Warner, R. J. Nicholas, H. L. Anderson, *Angew. Chem. Int. Ed.* **2011**, *50*, 2313.
- [45] R. Ahlrichs, M. Baer, M. Haeser, H. Horn, C. Koelmel, *Chem. Phys. Lett.* **1989**, *162*, 165.
- [46] A. D. Becke, *J. Chem. Phys.* **1993**, *98*, 5648.